JCBFM

Cortical atrophy and transcallosal diaschisis following isolated subcortical stroke

SAGE

Bastian Cheng[1], Philipp Dietzmann[1], Robert Schulz[1],
Marlene Boenstrup[1,2], Lutz Krawinkel[1], Jens Fiehler[3],
Christian Gerloff[1] and Götz Thomalla[1]

Abstract

Following acute ischemic stroke, isolated subcortical lesions induce gray matter atrophy in anatomically connected, yet distant cortical brain regions. We expand on previous studies by analyzing cortical thinning in contralesional, homologous regions indirectly linked to primary stroke lesions via ipsilesional cortical areas. For this purpose, stroke patients were serially studied by magnetic resonance imaging (diffusion tensor imaging and high-resolution anatomical imaging) in the acute (days 3–5) and late chronic stage one year after stroke. We analyzed changes of gray and white matter integrity in 18 stroke patients (median age 68 years) with subcortical stroke. We applied probabilistic fiber tractography to identify brain regions connected to stroke lesions and contralesional homologous areas. Cortical thickness was quantified by semi-automatic measurements, and fractional anisotropy was analyzed. One year after stroke, significant decrease of cortical thickness was detected in areas connected to ischemic lesions (mean -0.15 mm; 95% CI -0.23 to -0.07 mm) as well as homologous contralateral brain regions (mean -0.13 mm; 95% CI -0.07 to -0.19 mm). We detected reduced white matter integrity of inter- and intrahemispheric fiber tracts. There were no significant associations with clinical recovery. Our results indicate that impact of subcortical lesions extends to homologous brain areas via transcallosal diaschisis.

Introduction

In patients with ischemic stroke, a single lesion located in strategic subcortical brain areas such as the corticospinal tract regularly results in severe impairment of motor function. In the weeks and months after injury, secondary degeneration of white matter tracts can lead to structural and functional alterations located in distant and originally unaffected brain areas.[1] In a previous study combining white-matter tractography with surface-based cortical thickness analysis, we have identified a direct link of focal subcortical ischemic lesions to ipsilesional cortical atrophy at the early chronic stage three months after stroke.[2] We have attributed these findings to axonal degeneration as the underlying mechanism of cortical thinning in distant and primarily unaffected regions structurally connected to the focal stroke lesion. These changes fit well with

the concept of diaschisis after stroke (from Greek διάσχισις, "shocked through"), which generally describes the reduction of function, metabolism, and perfusion in brain areas distant to a cerebral lesion.

[1]Klinik und Poliklinik für Neurologie, Kopf- und Neurozentrum, Universitätsklinikum Hamburg-Eppendorf, Hamburg, Germany
[2]Human Cortical Physiology and Neurorehabilitation Section, National Institute of Neurological Disorders and Stroke, National Institutes of Health, Bethesda, MD, USA
[3]Klinik und Poliklinik für Neuroradiologische Diagnostik und Intervention, Universitätsklinikum Hamburg-Eppendorf, Hamburg, Germany

Corresponding author:
Bastian Cheng, Klinik und Poliklinik für Neurologie, Kopf- und Neurozentrum Universitätsklinikum Hamburg-Eppendorf, Martinistr. 52, Hamburg 20246, Germany.
Email: b.cheng@uke.de

During the acute stage after stroke, synaptic suppression in distant areas results in disruptions of brain metabolism and perfusion, whereas prolonged lack of afferent function may ultimately result in loss of structural integrity in distant, yet connected regions of the brain.[1,3–5]

In addition to ipsilesional changes, we previously reported indications of subtle cortical atrophy located on the contralesional hemsiphere as described previously by voxel-based morphometry (VBM) studies after stroke.[6,7] These changes appeared to follow a homologues pattern to ipsilesional, connected brain areas. In the current study, we expand on our previous investigation by prospectively analyzing the long-term impact of isolated subcortical lesions on cortical atrophy one year after stroke onset. We tested if selective cortical atrophy of brain areas connected to subcortical stroke lesions is observable in the late chronic stage one year after stroke, specifically in contralesional, homologous brain areas. In addition, we investigated the association of cortical changes with underlying structural integrity of intra- and interhemispheric white matter tracts as potential mediators. Lastly, we tested if changes of structural integrity relate to the degree of clinical recovery one year after stroke.

Materials and methods

Subjects

We prospectively enrolled patients with ischemic stroke and upper arm paresis. All patients were recruited three to five days after stroke onset via the Stroke Unit of our hospital if the following inclusion criteria were met: (1) acute stroke with upper limb motor deficit; (2) isolated acute subcortical ischemic stroke lesion and absence of obvious white matter lesions or lesions from previous stroke shown by magnetic resonance imaging (MRI); (3) written informed consent; (4) absence of severe neurological or non-neurological co-morbidity. We excluded patients with previous stroke, intracerebral hemorrhage or evidence of preexisting structural brain damage.

Results from clinical and MRI examinations were recorded on two time points (T1 and T2). First, during the acute stage (T1, days 3–5) and second, one year after stroke (T2). We have previously reported results from follow-up examinations three months after stroke in a subset of nine patients included in the current study.[2] The current study focusses on long-term changes of grey and white matter integrity; thus, only findings one year after stroke onset were considered for analysis. Patients with evident recurrent stroke at T2 were excluded (judged on clinical evidence, patient history and imaging findings). Clinical

examination included the National Institute of Health Stroke Scale (NIHSS), the modified Rankin scale and the Fugl-Meyer assessment of the upper extremity (UEFM). In addition, we measured grip force of the affected hand: the mean value (in kg) of three consecutive measurements was calculated as well as absolute and relative changes of all clinical parameters between both time points. Patients gave written informed consent according to the Declaration of Helsinki. The study was approved by the ethic committee of the medical council Hamburg, Germany.

Brain imaging

We acquired imaging data immediately following clinical examinations at each time point (T1 and T2). A 3T Siemens Skyra MRI scanner (Siemens, Erlangen, Germany) and 32-channel head coil was used to measure both diffusion-weighted and high-resolution T1-weighted anatomical images. For diffusion-weighted imaging, 75 axial slices were obtained covering the whole brain with gradients ($b = 1500$ s/mm^2) applied along 64 non-collinear directions with the sequence parameters: Repetition (TR) $= 10,000$ ms, echo time (TE) $= 82$ ms, field of view (FOV) $= 256 \times 204$, slice thickness (ST) $= 2$ mm, in-plane resolution (IPR) $= 2 \times 2$ mm. The complete dataset consisted of 2×64 b1500 images and additionally one b0 image at the beginning and one after the first 64 images. For anatomical imaging, a three-dimensional magnetization-prepared, rapid acquisition gradient-echo sequence (MPRAGE) was used with the following parameters: TR $= 2500$ ms, TE $= 2.12$ ms, FOV $= 240 \times 192$ mm, 256 axial slices, ST $= 0.94$ mm, IPR $= 0.94 \times 0.94$ mm. In addition, fluid-attenuated inversion recovery (FLAIR) sequences were acquired at T1 for delineation of ischemic lesions (TR $= 9000$ ms, TE $= 90$ ms, TI $= 2500$ ms, FOV $= 230 \times 230$ mm, ST $= 5$ mm IPR $= 0.7 \times 0.7$mm).

Data pre-processing

Diffusion-weighted images were analysed using the FSL software package 5.1 (http://www.fmrib.ox.ac.uk/fsl). All datasets were corrected for eddy currents and head motion. Fractional anisotropy (FA) maps were calculated fitting the diffusion tensor model at each voxel. Structural T1-weighted anatomical images were processed using the Freesurfer software package 6.0.0 with standard procedures and parameters that generate measurements of cortical thickness with high validity and reliability.[8–12] All images were visually inspected and data of insufficient quality (i.e. due to motion artefacts) excluded, specifically paying attention to accuracy of brain extraction. We applied careful manual
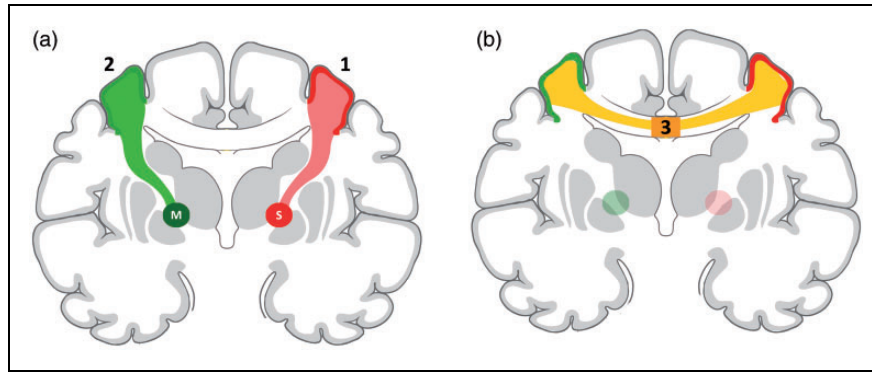
Figure 1. Schematic illustration of the methodological approach to gray and white matter region segmentations. (a) Reconstruction of white matter fiber tracts (light red) connecting the subcortical stroke lesion (S) with the cortical surface (dark red). Analogous reconstruction using a mirrored subcortical region (M) in the contralesional hemisphere. The unconnected cortex (no color) served as a control region. (b) Reconstruction of interhemispheric, transcallosal white matter tracts (light yellow) connecting cortical surfaces from (a) (dark red and dark green cortical regions). For transcallosal fiber integrity, values of fractional anisotropy were measured at the intersection with the corpus callosum (3, dark yellow).

corrections in cases of incorrect brain extraction results following recommendations from the online Freesurfer documentation. Registration of structural and diffusion datasets was achieved by using linear and non-linear transformation tools (FLIRT and FNIRT) implemented in FSL.[13]

Stroke lesion segmentation, intra- and interhemispheric probabilistic fiber tracking and definition of cortical regions of interest

A schematic representation of our analysis is shown in Figure 1. In summary, a semi-automated procedure using probabilistic fiber tracking was used to identify cortical areas connected and unconnected to the subcortical regions of interest (ROI). First, we defined these regions of interest comprising the original, acute stroke lesions (T1, stroke ROI, red) using the in-house software tool ANTONIA as described previously.[2] Each stroke ROI was then used as seed region for probabilistic fiber tracking to determine ipsilesional cortical brain areas structurally connected to the stroke ROI by white matter fiber tracts. Secondly, in order to study structural changes in homologous contralesional brain areas, an additional ROI was created at the contralesional hemisphere mirroring the stroke ROI at the interhemispheric midline (mirror ROI, green). Again, we determined connected, contralesional cortical brain regions using fiber tracking, this time starting at the mirror ROI. For both hemispheres, white matter tracts were reconstructed using probabilistic diffusion models and tractography (bedpost and probtrackx).[14,15] From each mask voxel (stroke ROI and mirror ROI), 10,000 samples were initiated through the probability fibre distribution of principle white

matter fibre directions with a curvature threshold of 0.2. Tracking was restricted to each hemisphere, respectively. Tracts ending at the brainstem or cerebellum were excluded to limit the analysis to fibers directly connecting the stroke and mirror ROI to the cortical surface. Resulting tract distributions were normalized in relation to the general connectivity profile in each individual patient. We applied a threshold of 100 samples (1% of 10,000 samples) as reported previously.[2] Regions where the tracts reached the white matter surface (as determined by Freesurfer) were defined as regions of interested. Cortical thickness (CT) was determined by the distance between the white-matter surface and the pial surface across the cortical mantle (Figure 1(a) and (b)). In addition to intrahemispheric probabilistic tracking, we reconstructed interhemispheric white matter tracts between the homologous, connected cortical areas to investigate the change of transcallosal fiber tract integrity. To this end, fibers connecting both connected cortical regions were reconstructed by reversely using each connected cortical region as seeding and end point for probabilistic fiber tracking (Figure 1(b), light yellow). For each patient, the resulting two individual tracts were binarized using a threshold of 1% of overall connectivity, summed and transferred to the dataset at T2 analogous to the analysis above. All probabilistic tracking and fiber reconstruction were carried out on data sets during the early stage (T1) after stroke, in line with pervious work.[2,16] This approach is inherently limited by the presence of perilesional edema confounding the probabilistic tracking algorithm in areas in close proximity to the primary lesion. However, the relatively small lesion volumes in our patients limit the extend of white matter distortions for probabilistic fiber tracking and visual inspection

revealed plausible results of the connecting white matter tracts. The alternative approach, i.e. using data from the chronic stage (T2), yields the issue of significant lesion shrinkage and loss connecting white matter fiber tracts contributing to a significant extend of false-negative results. We have therefore opted for the approach using data from the early stage after stroke (T1).

Measurement of cortical thickness

CT was measured in two cortical regions per hemisphere, leading to measurements from four cortical regions in total: Two regions connected and unconnected to the subcortical ROI in both the ipsi- and contralesional hemispheres (Figure 1). The cortical regions unconnected to the subcortical ROI served as control regions. We measured cortical thickness at both timepoints (T1 and T2) after stroke. Absolute values of cortical thickness were determined by the distance between the white matter and pial surface[9] and absolute change of cortical thickness between the two timepoints calculated for each ROI: Δ cortical Thickness $[mm] = (CT_{T2} - CT_{T1})$.

Analysis of white matter tract fractional anisotropy

In addition to cortical thickness, we measured values of fractional anisotropy (FA) at both time points as a marker for white matter integrity for both tracts connecting either the stroke or mirror lesion with the cortical surface (red and green tracts in Figure 1). Subcortical stroke and mirror ROI were dilated with a margin of 1 mm and excluded from both tracts. Resulting tracts were registered linearly to the diffusion dataset at T2. Mean FA values were then extracted from these tracts on both time points (T1, T2). For measurement of interhemispheric white matter tract integrity, FA values were calculated at the intersection of the interhemispheric tract and the corpus callosum defined by using a template from the standard 152MNI-space (Figure 1(b), dark yellow section marked with 3) at T1 and T2. To control for unspecific changes of callosal integrity after stroke, a control tract was reconstructed analogously between the primary visual cortices (V1) of both hemispheres analogously to the main tract of interest. This tract was chosen due to its distance to the transcallosal fibers of interest located at the middle and anterior part of the corpus callosum. Furthermore, lesion distribution spared the posterior arterial territory in our patients and significant alterations of white matter connectivity in these areas were unlikely. Again, mean FA values were measured at the intersection of the control tract with the corpus callosum at T1 and T2.

Statistical analysis

For descriptive statistics, mean or median values with 95% confidence intervals (95% CI) or interquartile range (IQR) were calculated as appropriate.

We applied a univariate linear model (ANOVA) to test for significant changes of cortical thickness using the absolute thickness on T1 and T2. The model included the following factors: time of examination (T1 or T2), region of interest (ROI connected or not connected to the lesion) as well as the interaction between time and ROI. We tested for significant correlations between changes of cortical thickness and white matter integrity (FA-values) in individual ROI and tracts using a two-tailed Spearman's test.

Changes of clinical parameters were calculated: Change of NIHSS over one year = $NIHSS_{T2}$ – $NIHSS_{T1}$. Changes were calculated for the UEFM score and grip strengths (affected hand) accordingly. PC of cortical thickness and changes of clinical parameters were correlated using a two-tailed Spearman's rank correlation coefficient. Similarly, absolute changes of FA values in reconstructed tracts (ipsilesional, contralesional and interhemispheric) were correlated with change of clinical parameters. All statistical analyses were done in SPSS 25.0 (IBMCo., Somers, NY, USA). For visual representations (Figures 2 and 3), all imaging data were flipped to the left hemisphere.

Results

In total, 27 patients were included in our study. Of those, one patient was excluded from analyses due to insufficient image quality of the diffusion imaging data at the follow-up examination. In addition, one patient was unable to participate at follow-up examination after one year due to implantation of a cardiac event recorder. Seven patients did not respond to our invitation at follow-up. Data from the remaining 18 patients were used for analyses. Of those, nine were included in our previous study reporting results of focal cortical thinning three months after stroke.[2] Median duration post-stroke was four days (range: 3–5 days) at T1 and 361 days (range: 341–409 days) at T2. Thirteen patients (72 %) were male, median age was 68 (IQR 47–81 years). Stroke lesions were located at the left hemisphere in 11 patients (61%), mean lesion volume was 4.4 ml (95% CI 1.6–5.8 ml). At T1, median NIHSS was 4 (IQR 2–6). All patients recovered after one year with a median NIHSS of 0 (IQR 0–2) at T2. Table 1 summarizes the clinical characteristics of our patients.

Figure 2 illustrates the distribution of subcortical stroke lesions and connected cortical areas represented on a standard volumetric template and hemispheric surface provided by Freesurfer (fsaverage template),
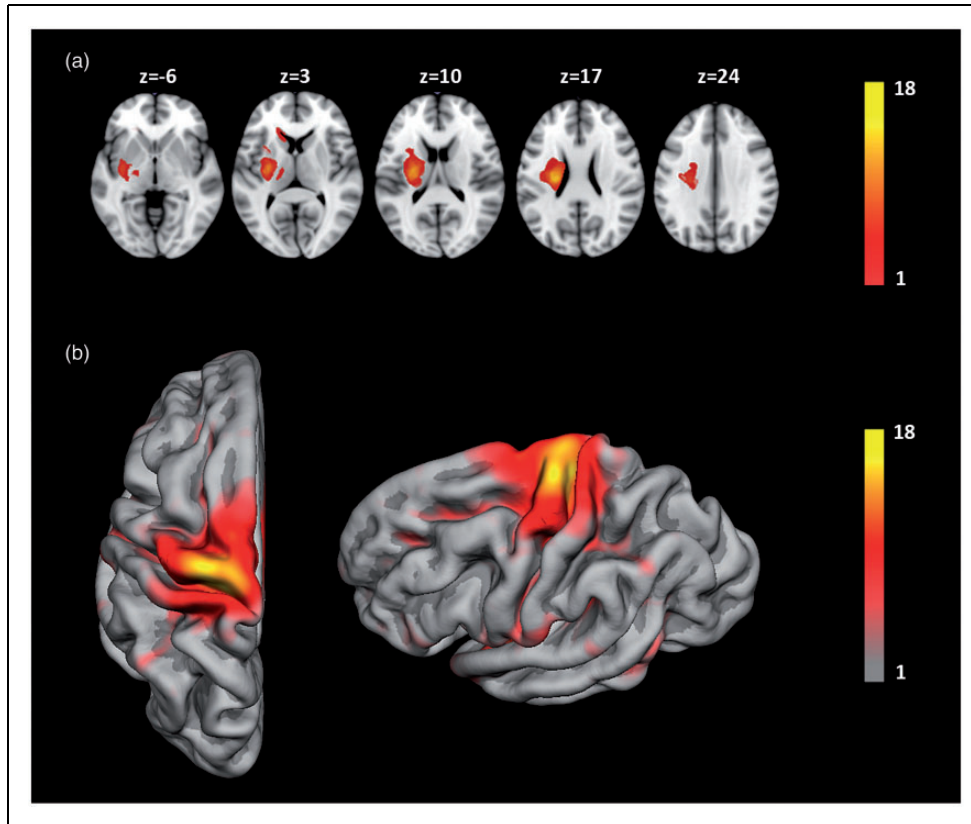
Figure 2. (a) Overlay lesion plot of segmented stroke lesions of all patients (*n* = 18), z-coordinates correspond to the standard MNI152 brain template. (b) Surface map of cortical areas connected to subcortical stroke lesions. Overlay color indicates number of patients (see color bar). For illustrative purposes, all lesions were flipped to the left hemisphere.
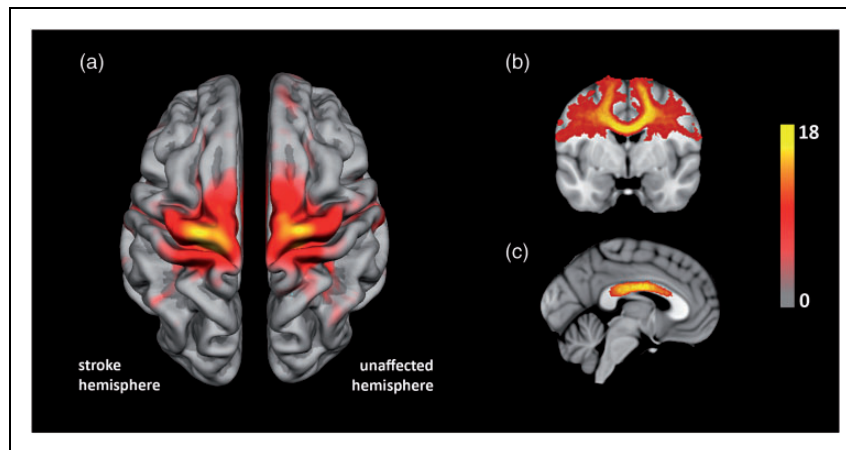
Figure 3. (a) Illustration of cortical areas connected to subcortical stroke lesions ("stroke hemisphere") and mirrored subcortical regions ("unaffected hemisphere"). Overlay color indicates number of patients (see color bar). (b) Representative brain section illustrating the frequency of individual inter-hemispheric white matter tracts connecting homologous cortical areas. (c) Distribution of white matter fiber tracts at midline level projected on the corpus callosum shown on a standard MNI152 brain template.

respectively. Due to the inclusion criteria of present upper extremity motor deficits in all our patients, stroke lesions were mainly connected to cortical areas involving motor functions located on the precentral, postcentral and superior frontal cortex (Figure 2(b)). On a cytoarchitectonic level, these regions correspond to cranial parts of Brodmann Areas 3, 4, 6 and 8. Fiber tracking starting from the contra-lesional mirror ROI

resulted in a distribution of cortical areas symmetrical to the lesion hemisphere as demonstrated in Figure 3(a). Note that for illustrative purposes, all surfaces and subcortical lesions were flipped to the left hemisphere.

Changes of cortical thickness

Cortical regions connected to subcortical stroke lesions and mirror regions were defined successfully in all patients. Application of a threshold of 1% to the overall probabilistic fiber distribution resulted in two cortical regions of comparable size on both the ipsi- and contralesional hemisphere (mean surface area of $51.0\,cm^2$ and $52.8\,cm^2$, respectively). In the ipsilesional hemisphere, thickness of areas connected to the stroke lesion decreased by $-0.15\,mm$ (95% CI -0.23 to $-0.07\,mm$) within the first year after stroke. In addition, thickness of cortical areas connected to the mirror region at the contralesional hemisphere decreased by $-0.13\,mm$ (95% CI -0.07 to $-0.19\,mm$). Cortical thinning was also present in unconnected areas on both hemispheres, albeit at a lower rate (Table 2 and Figure 4). Analysis from the univariate linear model (ANOVA) demonstrated significant effects of time (T1 or T2; $F = 12.5$, $p < 0.001$), region of interest (ROI; connected or not connected; $F = 20.4$; $p < 0.001$) as well as the interaction time $\times$ ROI ($F = 3.0$; $p = 0.047$) on cortical thickness. There was a decrease of cortical thickness specifically located in areas connected to the lesion/mirror region (compared to the unconnected cortical areas, Figure 4).

Analysis of white matter integrity

We first analyzed integrity of ipsilesional white matter fiber tracts connecting the stroke lesion to the cortical surface as well as integrity of analogous fiber tracts at the contralesional hemisphere. No differences of FA values were observed at T1 between the ipsi- and contralesional fiber tracts. White matter integrity of the ipsilesional fiber tract declined significantly demonstrated by lower FA values at T2 (0.39; 95% CI 0.37–0.41) compared to T1 (0.44; 95% CI 0.42–0.46; $p = 0.008$). In contralesional fiber tracts, white matter integrity remained almost unchanged between T1 and T2 (Table 3). As a second step, callosal FA values were measured at the intersection with the interhemispheric fiber tracts connecting cortical regions on the ipsi- and contralesional hemispheres. Figure 3(c) illustrates the distribution of interhemispheric fiber tracts intersecting the corpus callosum, which were primarily located at the sensory and motor callosal sections extending to anterior, premotor sections as previously defined by a DTI-based atlas (Sections II, III and IV of the corpus callosum classified by Hofer and Frahm[17]). FA values of transcallosal tracts between cortical regions connected to the stroke lesion and mirror lesion declined significantly between T1 (0.67; 95% CI 0.64–0.68) and T2 after one year (0.63; 95% CI 0.61–0.64, $p = 0.032$). In contrast, no changes of FA values were observed at the intersection with the control tract between both primary visual cortices located at the posterior end of the corpus callosum (section V based on the atlas of Hofer and Frahm[17]).

Correlation with clinical parameters and white/grey matter integrity

Changes of cortical thickness did not correlate significantly with the rate of clinical recovery (absolute

**Table 1.** Overview of clinical data at days 3–5 (T1) and one year (T2) after stroke.

	T1	T2
Age (mean, IQR)	68 (47–81)	–
NIHSS (median, IQR)	4 (2–6)	0 (0–2)
UEFM (mean, 95% CI)	47.1 (41.5–52.8)	56.9 (52.2–61.1)
Grip strength [kg] (mean, 95% CI)	17.8 (14.8–20.7)	29.3 (25.6–32.9)

IQR: Interquartile range; CI: confidence interval; NIHSS: National Institutes of Health Stroke Scale; UEFM: Fugl-Meyer Assessment of sensorimotor function. Grip strength was measured in the affected hand.

Table 2. Absolute change of cortical thickness one year after stroke.

	Connected cortex		Unconnected cortex	
	Mean [mm]	95% CI (up/low)	Mean [mm]	95% CI (up/low)
Ipsilesional hemisphere	−0.15	−0.23/−0.07	−0.04	−0.08/−0.01
Contralesional hemisphere	−0.13	−0.19/−0.07	−0.04	−0.09/0.01

Note: Absolute values in millimeter are reported in areas connected and unconnected to subcortical stroke and mirrored contralesional regions. Mean values and 95% confidence intervals are shown.
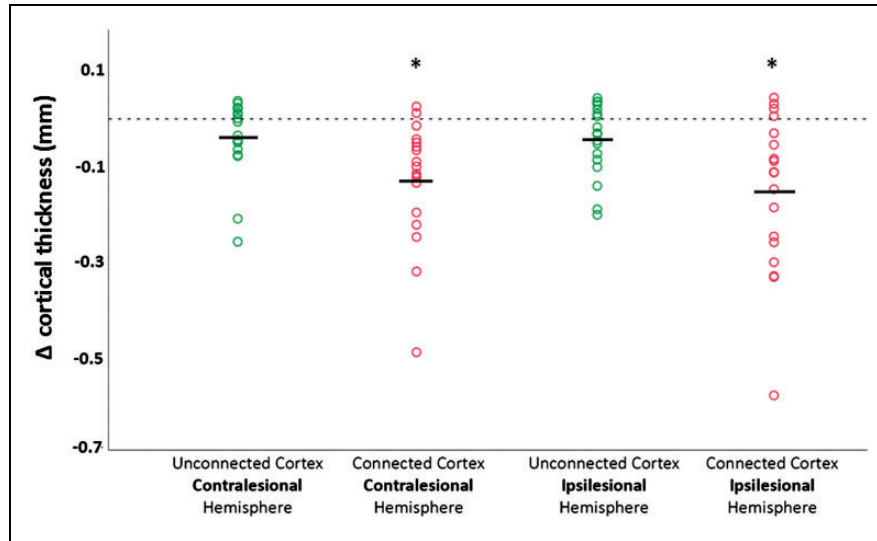
Figure 4. Individual values (circles) and mean absolute change (Δ Focal cortical thickness [mm]) of cortical thickness one year after stroke in areas connected and unconnected to subcortical stroke and mirrored contralesional regions. Unconnected areas are shown in green, connected areas are shown in red. * Analysis from the univariate linear model (ANOVA) demonstrated significant effects of time (T1 or T2; F = 12.5, $p < 0.001$), region of interest (ROI; connected or not connected; F = 20.4; $p < 0.001$) as well as the interaction time and ROI (F = 3.0; $p = 0.047$) with lower cortical thickness in areas connected to the subcortical stroke and mirrored contralesional regions.

Table 3. Fractional anisotropy (FA) values in reconstructed white matter fiber tracts.

Region of measurement	T1	T2	p^*
Lesion tract	**0.44 (0.42–0.46)**	**0.39 (0.37–0.41)**	**0.008**
Mirror tract	0.44 (0.43–0.46)	0.43 (0.42–0.45)	0.712
Interhemispheric tract at corpus callosum	**0.67 (0.64–0.68)**	**0.63 (0.61–0.64)**	**0.032**
V1–V1 tract at corpus callosum	0.69 (0.67–0.72)	0.69 (0.66–0.71)	0.501

Note: Longitudinal results on days 3–5 (T1) and one year after stroke (T2) are shown. See also Figure 1 illustrating areas of measurement. V1–V1 corresponds to interhemispheric fiber tracts connecting primary visual cortices on both hemispheres. *p-values resulting from Mann–Whitney–U-Test between T1 and T2.
Significant differences ($p<0.05$) of FA between T1 and T2 are marked with bold values.

change of clinical scores) over one year measured by the NIHSS, UEFM and grip strength of the affected hand. Similarly, integrity of intra- and interhemsipheric white matter fiber tracts did not correlate with clinical measurements over time. We did not observe significant correlations between measures of white matter (FA) and grey matter (change of cortical thickness) integrity (see Supplementary Material).

Discussion

Our study yielded three major results: First, specific focal atrophy of cortical brain areas connected to the subcortical stroke is found in the chronic phase one year after ischemic stroke. Second, we detected significant decreases of cortical thickness in the contralesional hemisphere in cortical regions homologous to brain areas connected to the primary lesion side. Lastly, we found evidence of altered integrity of white matter fiber tracts connecting the stroke lesion to the cortical surface, and in sections of the corpus callosum traversed by interhemispheric connections between connected cortical brain areas and homologous regions. These changes, however, were not found to be associated with clinical recovery after stroke in our patients.

Our findings of reduced cortical thickness in brain areas connected to the subcortical stroke lesion add to the increasing amount of evidence that confined, focal white matter injuries induce remote alterations of gray matter integrity as observed in experimental animal models, as well as structural imaging studies of patients with vascular or demyelinating brain injury.[7,18,19]

Complimentary to observations based on shorter time intervals (i.e. three and six months) after stroke,[2,16] we demonstrate that pronounced, lesion-dependent and specific regional cortical atrophy is a consistent finding in subcortical stroke after one year. In our population, cortical thinning in connected cortical areas occurred at an extend of 5% after one year, which clearly exceeds previous estimates of annual cortical thinning in elderly, healthy individuals that ranges between 0.3% and 3% per year, depending on the average age of the studied population.[20,21] This finding supports the concept of specific, lesion-dependent mechanisms underlying cortical atrophy beyond the global rate of general atrophic processes observed in healthy aging.

In our study, the pattern of connected cortical surface areas involved a cortical network of primary and secondary motor control located on the precentral, postcentral and superior frontal gyrus. This distribution results from our inclusion criteria of upper extremity motor deficits and the subsequent involvement of the pyramidal tract by the stroke lesion. We explain the specific atrophy by retrograde degeneration of underlying white matter tracts disrupted by the subcortical stroke lesion. In line with this hypothesis and previous findings from stroke imaging studies,[16,22] loss of microstructural integrity in white matter fiber tracts, connecting to the lesion, was observed in our patients as signified by a significant decrease of fractional anisotropy after one year. However, other factors, such as diffusely distributed cortical hypometabolism found in previous studies of diaschisis after subcortical stroke[23,24] might as well have contributed to these changes via transneuronal mechanism at the ipsi- and contra-lesional hemisphere.

In addition to regional cortical atrophy at the lesioned hemisphere, we observed cortical thinning on the contralesional hemisphere in areas linked with the spatially corresponding subcortical region. Similar to changes observed on the lesioned hemisphere, significant cortical atrophy occurred exclusively in connected cortical regions, whereas unconnected areas did not display significant changes. Interestingly, we did not detect significant cortical thinning during the early chronic stage after stroke in our previous, methodically analogous, analysis, although a trend to contralesional atrophy was apparent.[2] Taken together, these findings indicate that gray matter atrophy of homologous, contralesional brain areas might occur during the late chronic time span after isolated subcortical stroke. As of today, only few studies have demonstrated cortical atrophy contralesional to the ischemic injury after stroke. Extensive global decreases in gray matter volumes of contralesional gray matter one to four years after stroke were shown by VBM, specifically at the (contralesional) pre- and postcentral gyrus.[25,26]

Secondary reductions of contralesional insular gray matter volumes have furthermore been described as early as 12 weeks after stroke in data from VBM analysis.[6] These findings are supported by data from experimental animal studies demonstrating a spatial pattern of cortical thinning in the contralesional hemisphere mirroring the atrophy of the healthy hemisphere in a forelimb motor cortex stroke model.[7] It has been hypothesized that these changes in the contralesional hemisphere are mediated by secondary neuroinflammatory response or neurodegeneration. However, given previous findings on diaschisis after stroke, we would argue that mechanisms involving the secondary degeneration of transcallosal fibers are much more likely candidates to explain our findings.

In this study, we present novel data from the combined analysis of gray and white matter integrity, which point towards a possible mechanism underlying contralesional cortical changes. Focal cortical thinning of homologues, contralesional brain areas was associated with structural disintegration of the corpus callosum, specifically in sections crossed by fiber tracts connecting contralesional cortical regions to brain areas directly linked to the stroke lesion. These intersections were located in the sensory, motor and premotor sections of the corpus callosum, in line with imaging studies in humans[17] as well as anatomical tracer work in non-human primates that demonstrate transcallosal white matter tracts connecting primary and secondary cortical motor areas of both hemispheres.[27,28] Based on our results, we propose that the observed atrophy of contralesional homologous cortical areas in our patients one year after stroke is mediated by the degeneration of interhemispheric, transcallosal white matter tracts, secondary to ipsilesional cortical changes.

We can only hypothesize on the pathophysiological causes underlying this proposed "transcallosal diaschisis" in our group of patients with isolated subcortical stroke. As a main mechanism, we suggest that isolated subcortical lesions could induce contralesional cortical degeneration via an indirect pathway through interneurons at the ipsilesional hemisphere that have an intermediary function by inducing apoptosis in neurons following loss of synaptic input.[29] After subcortical stroke, disintegration of ipsilesional white matter tracts connecting to the cortical surface may propagate such effects by retrograde degeneration of pyramidal cell bodies in layer V and subsequent (anterograde) degeneration of cell bodies of interhemispheric neurons in layer III via cortical inhibitory GABA interneurons.[30] The localized and specific degeneration of gray and white matter (reduced FA and cortical thinning) in our study would lend support to his hypothesis. Alternatively, functional under-activation of primary

and secondary motor areas could contribute to a non-use cortical atrophy in line with observations of co-localized structural and functional plasticity in the somatosensory cortex after stroke. Analogous to co-localized over-activation and increases of cortical thickness,[31] the opposite mechanism of loss of excitatory inputs from the affected cerebral hemisphere could in turn induce contralesional cortical atrophy conveyed by the corpus callosum. Furthermore, diminished inter-hemispheric resting state functional connectivity is a prominent feature observed during the acute and sub-acute period after stroke,[32] although a gradual normalization toward the pre-stroke functional connectivity pattern tends to occur specifically in well-recovered patients. Thus, one might speculate that diminished callosal integrity as observed in our patients represents a long-term structural imprint of functional disconnection between homotopic cortical areas after subcortical stroke. However, these hypotheses cannot be substantiated by our data and further studies combining structural and functional imaging data are needed.

In our study, neither remote changes of cortical thickness nor integrity of subcortical white matter tracts were associated with clinical parameters of motor function. Thus, we cannot link our findings to the degree of recovery after subcortical stroke. However, these negative findings are consistent with results from previous studies focusing on the atrophy of remote, yet connected cortical areas after stroke.[33] In addition, recent work on thalamic diaschisis in terms of local hypometabolism after stroke has not been shown to be associated with clinical outcomes,[34] similar to the lack of clinical correlates of falling contralesional hemispheric oxygen metabolism after stroke over time.[35] Thus, our findings would be in line to the hypothesis that ipsi- and contralesional hemispheric diaschisis and atrophy after stroke appear largely an epiphenomenon with no clinical implication. Thus, the observed consequences of secondary neurodegeneration would develop, while patients actually improve motor function after stroke, rendering it plausible that the reorganization subserving recovery takes place in alternative circuits of the damaged neural network. In terms of potential methodological limitations, lack of clinical associations may also relate to the relatively small sample size of our study, which has to be considered as a limitation. Furthermore, one has to consider technical limitations of established methods for measurement of cortical thickness. Specifically, we cannot rule out the possibility that part of the atrophy seen in the ipsilesional, connected ROI may reflect resolution of subacute edema travelling along the connecting fibers, although these alterations – if severe – would be detectable by alterations of the signal intensity of diffusion weighted images. Lastly, although our methodological approach planned for the unconnected cortices as intrinsic control regions, the lack of data from healthy controls is an additional limitation.

In conclusion, we demonstrated that atrophy of remote cortical areas connected to single subcortical lesions remains prominent one year after ischemic stroke. At the same time, contralesional cortical atrophy is detectable in homologous cortical areas. These changes are potentially mediated by degeneration of transcallosal white matter tracts. Our findings underline the long-range impact of focal subcortical brain lesions on the structural integrity of networks involving both directly and indirectly connected cortical areas.

Authors' contributions

Bastian Cheng made substantial contributions to the design, and acquisition of data, analysis and interpretation of data and drafting the article as well as revising it critically for important intellectual content.

Philipp Dietzmann made substantial contributions to the design and analysis and interpretation of data and drafting the article as well as revising it critically for important intellectual content.

Robert Schulz made substantial contributions to the design and acquisition of data, interpretation of data, drafting this article and revising the manuscript critically for important intellectual content.

Marlene Boenstrup made substantial contributions to acquisition of data, interpretation of data, drafting this article and revising the manuscript critically for important intellectual content.

Lutz Krawinkel made substantial contributions to acquisition of data, interpretation of data, drafting this article and revising the manuscript critically for important intellectual content.

Jens Fiehler made substantial contributions to acquisition of data and revising the manuscript critically for important intellectual content.

Christian Gerloff made substantial contributions to the design, interpretation of data, drafting this article and revising the manuscript critically for important intellectual content.

Götz Thomalla made substantial contributions to design and acquisition of data, interpretation of data and revising the manuscript critically for important intellectual content.

All authors approved the version to be published.

Declaration of conflicting interests

The author(s) declared the following potential conflicts of interest with respect to the research, authorship, and/or

Supplemental material

Supplemental material for this paper can be found at the journal website: http://journals.sagepub.com/home/jcb

References

1. Carrera E and Tononi G. Diaschisis: past, present, future. *Brain* 2014; 137: 2408–2422.
2. Cheng B, Schulz R, Bönstrup M, et al. Structural plasticity of remote cortical brain regions is determined by connectivity to the primary lesion in subcortical stroke. *J Cereb Blood Flow Metab* 2015; 35: 1507–1514.
3. Pantano P, Baron JC, Samson Y, et al. Crossed cerebellar diaschisis. *Brain* 1986; 109: 677–694.
4. Feeney DM and Baron JC. Diaschisis. *Stroke* 1986; 17: 817–830.
5. Baron JC. Depression of energy metabolism in distant brain structures: studies with positron emission tomography in stroke patients. *Semin Neurol* 1989; 9: 281–285.
6. Dang C, Liu G, Xing S, et al. Longitudinal cortical volume changes correlate with motor recovery in patients after acute local subcortical infarction. *Stroke* 2013; 44: 2795–2801.
7. Karl JM, Alaverdashvili M, Cross AR, et al. Thinning, movement, and volume loss of residual cortical tissue occurs after stroke in the adult rat as identified by histological and magnetic resonance imaging analysis. *Neuroscience* 2010; 170: 123–137.
8. Dale AM, Fischl B and Sereno MI. Cortical surface-based analysis. I. Segmentation and surface reconstruction. *Neuroimage* 1999; 9: 179–194.
9. Fischl B and Dale AM. Measuring the thickness of the human cerebral cortex from magnetic resonance images. *Proc Natl Acad Sci U S A* 2000; 97: 11050–5.
10. Fischl B. FreeSurfer. *Neuroimage* 2012; 62: 774–781.
11. Han X, Jovicich J, Salat D, et al. Reliability of MRI-derived measurements of human cerebral cortical thickness: the effects of field strength, scanner upgrade and manufacturer. *Neuroimage* 2006; 32: 180–94.
12. Reuter M, Rosas HD and Fischl B. Highly accurate inverse consistent registration: a robust approach. *Neuroimage* 2010; 53: 1181–96.
13. Jenkinson M, Beckmann CF, Behrens TEJ, et al. Fsl. *Neuroimage* 2011; 62: 782–790.
14. Behrens TEJ, Berg HJ, Jbabdi S, et al. Probabilistic diffusion tractography with multiple fibre orientations: what can we gain? *Neuroimage* 2007; 34: 144–155.
15. Smith SM, Jenkinson M, Woolrich MW, et al. Advances in functional and structural MR image analysis and implementation as FSL. *Neuroimage* 2004; 23(Suppl 1): S208–S219.
16. Duering M, Righart R, Wollenweber FA, et al. Acute infarcts cause focal thinning in remote cortex via degeneration of connecting fiber tracts. *Neurology* 2015; 84: 1685–1692.
17. Hofer S and Frahm J. Topography of the human corpus callosum revisited – comprehensive fiber tractography using diffusion tensor magnetic resonance imaging. *Neuroimage* 2006; 32: 989–994.
18. Steenwijk MD, Daams M, Pouwels PJW, et al. Unraveling the relationship between regional gray matter atrophy and pathology in connected white matter tracts in long-standing multiple sclerosis. *Hum Brain Mapp* 2015; 36: 1796–1807.
19. Koch P, Schulz R and Hummel F. Structural connectivity analyses in motor recovery research after stroke. *Ann Clin Transl Neurol* 2016; 3: 233–244.
20. Jiang J, Sachdev P, Lipnicki DM, et al. NeuroImage A longitudinal study of brain atrophy over two years in community-dwelling older individuals. *Neuroimage* 2014; 86: 203–211.
21. Shaw ME, Sachdev PS, Anstey KJ, et al. Age-related cortical thinning in cognitively healthy individuals in their 60s: the PATH through life study. *Neurobiol Aging* 2016; 39: 202–209.
22. Liang Z, Zeng J, Liu S, et al. A prospective study of secondary degeneration following subcortical infarction using diffusion tensor imaging. *J Neurol Neurosurg Psychiatry* 2007; 78: 581–586.
23. Pappata S, Mazoyer B, Dinh ST, et al. Effects of capsular or thalamic stroke on metabolism in the cortex and cerebellum: a positron tomography study. *Stroke* 1990; 21: 519–524.
24. Kushner M, Alavi A, Reivich M, et al. Contralateral cerebellar hypometabolism following cerebral insult: a positron emission tomographic study. *Ann Neurol* 1984; 15: 425–434.
25. Yin D, Yan X, Fan M, et al. Secondary degeneration detected by combining voxel-based morphometry and tract-based spatial statistics in subcortical strokes with different outcomes in hand function. *AJNR Am J Neuroradiol* 2013; 34: 1341–1347.
26. Kraemer M, Schormann T, Hagemann G, et al. Delayed shrinkage of the brain after ischemic stroke: preliminary observations with voxel-guided morphometry. *J Neuroimaging* 2004; 14: 265–272.
27. Dancause N, Barbay S, Frost SB, et al. Interhemispheric connections of the ventral premotor cortex in a new world primate. *J Comp Neurol* 2007; 505: 701–715.
28. Fang PC, Stepniewska I and Kaas JH. Corpus callosum connections of subdivisions of motor and premotor cortex, and frontal eye field in a prosimian primate, Otolemur garnetti. *J Comp Neurol* 2008; 508: 565–578.
29. Koliatsos VE, Dawson TM, Kecojevic A, et al. Cortical interneurons become activated by deafferentation and instruct the apoptosis of pyramidal neurons. *Proc Natl Acad Sci U S A* 2004; 101: 14264–14269.
30. Avanzino L, Teo JTH and Rothwell JC. Intracortical circuits modulate transcallosal inhibition in humans. *October* 2011; 1: 99–114.

31. Schaechter JD, Moore CI, Connell BD, et al. Structural and functional plasticity in the somatosensory cortex of chronic stroke patients. *Brain* 2006; 129: 2722–2733.

32. Thiel A and Vahdat S. Structural and resting-state brain connectivity of motor networks after stroke. *Stroke* 2015; 46: 296–301.

33. Duering M, Righart R and Wollenweber FA. Acute infarcts cause focal thinning in remote cortex via degeneration of connecting fiber tracts. *Neurology* 2015; 84: 1685–1692.

34. Reidler P, Thierfelder KM, Fabritius MP, et al. Thalamic diaschisis in acute ischemic stroke. *Stroke* 2018; 49: 931–937.

35. Iglesias S, Marchal G, Rioux P, et al. Do changes in oxygen metabolism in the unaffected cerebral hemisphere underlie early neurological recovery after stroke? A positron emission tomography study. *Stroke* 1996; 27: 1192–1199.